Formation Mechanism of Microvoids and Microcracks of Poly(vinyl chloride) Under an Artificial Aging Environment

Jun Xiang, Jiliang Wang, Xiaofeng Chen, Jingxin Lei

State Key Laboratory of Polymer Materials and Engineering, Polymer Research Institute of Sichuan University, Chengdu 610065, People's Republic of China

Received 16 March 2011; accepted 2 September 2011
DOI 10.1002/app.35562
Published online 17 December 2011 in Wiley Online Library (wileyonlinelibrary.com).

ABSTRACT: Degradation behaviors of both the unplasticized and plasticized poly(vinyl chloride) (UPVC and PPVC) under an artificial accelerating aging condition were extensively studied. The dependence of mechanical properties, average molecular weight (MW), and surface morphology of the earlier PVC on aging time was investigated by tensile tests, gel penetrate chromatogram (GPC), and scanning electron microscope (SEM), respectively. Fourier transform infrared and ultraviolet (UV)–visible spectroscopy were used to evaluate the probable formation of both the oxygen-containing groups and the conjugated sequences during aging. The results reveal that UPVC is much easier to be degraded than PPVC under the same testing conditions. The irradiated surface is detected to change from an even topology into a rough topology initially, and then follows the appearance of many voids even cracks in the SEM morphology. During the aging process, oxygen-containing groups and conjugation of PVC molecular chains around the cracks are observed, and noticeably increase with aging time. However, visible difference of the corresponding MWs of PVC before and after aging is not detected. Moreover, a novel degradation mechanism nearly related to the formation of microvoids and microcracks based on the cohesion energy of groups along PVC molecular chains is developed and semiquantitatively discussed. It is detected that the formation of microvoids and microcracks is attributed to both the thermodynamic changes of PVC backbone during the aging and the aggregation of oxygen-containing groups with relatively large volumes. © 2011 Wiley Periodicals, Inc. J Appl Polym Sci 125: 291–299, 2012

Key words: poly(vinyl chloride); plasticization; aging; degradation; cohesion energy

INTRODUCTION

Poly(vinyl chloride) (PVC) is one of the most widely used commercial polymeric materials due to its low cost, antierosion capacity, flame resistance, and long-term stability.[1–3] It can be easily changed from a thorough hard material into a flexible material by adding amounts of plasticizer such as dioctyl phthalate (DOP). Nevertheless, "permanence" may be regarded as the most important aspect for a product, whether this permanence relates to dimensional stability, mechanical properties or environment (resistance to aging). In this regard, their comprehensive stabilities, especially the change of color and mechanical property, related to outdoor conditions and aging time need to be authenticated.

Many efforts have been done to simulate the dependence of both the macrocosmic and microcosmic structure of PVC molecular chains on aging conditions in the accelerating aging process.[4–10] It is convinced that the photo-dehydrochlorination of PVC is dominated in the initial aging step. Subsequently, double bonds even conjugated polyenes are formed, which will directly lead to the discoloration of polymer. After a long-term aging, ample surface defects are detected and both the physical and mechanical properties are found to evidently deteriorate, indicating an apparent reduction of stability. Moreover, both the conjugated polyenes and the oxygen-containing molecular sequences can be crosslinked by the elimination of corresponding free radicals, which partially increases the molecular weight (MW) of molecular sequences. Such crosslinking is also likely to reduce the mechanical properties due to the increase of incompatibility between crosslinked PVC molecular chains and plasticizer molecules. However, the most important factor directly related to the practical application of materials is the formation of microcosmic voids and cracks in the initial stage, because it is likely to result in reducing both the physical and mechanical properties.

Recently, Ito and Nagai have reported that the formation of surface defects is attributed to the elimination of inorganic filler and plasticizer, and to the aggregation of molecular chains in interfacial layer.[11]

Correspondence to: J. Lei (jxlei@scu.edu.cn).

TABLE I
Recipe of UPVC and PPVC

	UPVC (phr)	PPVC (phr)
PVC powder	100	100
Stabilizer	4	4
DOP	0	60

However, microvoids and microcracks are also detected in the specimen without inorganic fillers.[12,13] It indicates that an internal factor on molecular level, which directly leads to the formation of microvoids and microcracks during the aging process, is unclear.

In this article, we have investigated the formation and growth of microvoids and microcracks with aging time by scanning electron microscope (SEM). Then the change of both the intensity of oxygen-containing groups and the conjugated polyenes around microvoids and microcracks, and their relationships are extensively evaluated. A new mechanism, which can semiquantitatively interpret the formation diversity of microvoids and microcracks between unplasticized PVC (UPVC) and plasticized PVC (PPVC) is developed and discussed.

EXPERIMENTAL

Materials

Commercial PVC (type: SG-3, $K = 68$) was supplied by Tianyuan Co. (Yibing, China). DOP was industrially pure, and purchased from Qilu Petrochemical Co. (Shandong, China). Compound stabilizer Baeropan (type: SMS-318) was supplied by Bearlocher Corp. (Lingen, Germany). All the other chemicals used were analytically pure without further purification.

Artificial accelerating aging test

Tables I and II showed the recipe and test conditions of accelerating aging of both the PVC and UPVC, respectively. For preparing the testing specimen, PVC powder, plasticizer, and stabilizer were premixed in a high-speed mixing chamber at room temperature for 5 min, and the mixing speed was 1500 rpm. The resulting mixture was dried at 70°C for a given time (about 2 h), and then used for molding by a calendar roll [type: SK-160B, size: 160 mm × 320 mm (diameter × length), Shanghai, China] at 170–180°C in the form of 0.5-mm-thick sheet. After that, the sheet was again molded by compression molding at 180°C to form the 1-mm-thick flake. The dumbbell samples (30 mm × 3 mm × 0.5 mm) which were cut from the earlier flake were used for the accelerating aging and other characterizations.

Characterization

SEM analysis

SEM micrographs of the surfaces of specimen with aging time were studied by using a JEOLJSM-5900LV SEM (Japan) set to an accelerated voltage of 20 kV. The SEM specimens were gold-sputtered prior to observation.

Attenuated total reflection (ATR)-Fourier transform infrared (FTIR) analysis

The intensity of oxygen-containing groups of the unaged specimen and the neighboring regions around microcracks with different aging time was investigated by using a Nicolet 560 FTIR spectrometer at a resolution of 4 cm^{-1}. The scanning range was altered from 400 to 4000 cm^{-1}.

Ultraviolet (UV)–visible measurement

UV–visible spectra of the specimen with different aging time were collected by using an UV-2100 (Shimadzu Corp., Japan) UV–visible spectrometer, and tetrahydrofuran (THF) was used as the solvent.

Gel penetrate chromatogram (GPC) measurement

The change of the MW of specimens with aging time was measured with an Agilent 1100 GPC (Agilent Technology Co.) at 30°C using the solvent of THF. The flow speed of the solution was 1 ml/min, and two polystyrene separators with individual particle sizes of 10 Å and 100 Å were used.

Tensile tests

After different aging time, the specimens were used for the tensile tests by using an Instron4302 set the tensile rate of 50 and 100 mm/min for UPVC and PPVC, respectively.

TABLE II
Accelerating Aging Conditions

Light source	Gallium iodide lamp
Wavelength (nm)	320–450
Temperature (°C)	50
Irradiance (mJ/cm^2)	46

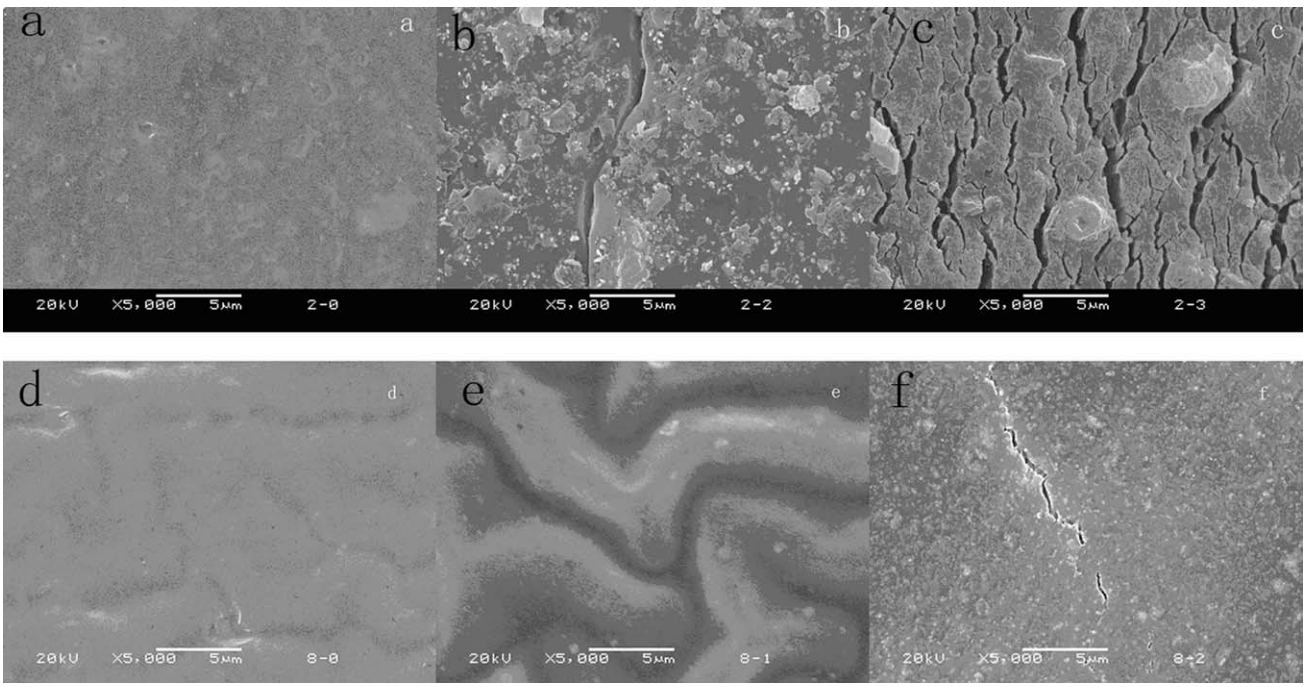

Figure 1 Surface morphology of the sample with different aging time: (a) 0 h, (b) 4 h, and (c) 8 h for UPVC; and (d) 0 h, (e) 4 h, and (f) 8 h for PPVC.

RESULTS AND DISCUSSION

SEM results

Surface morphologies of both the UPVC and PPVC with different aging time are shown in Figure 1(a–f). A relatively even and smooth topology is detected for both them at the very beginning of aging [Fig. 1(a,d)]. With increasing the aging time to 4 h, in the case of the UPVC, a large number of microvoids, whose size ranges from 200 to 400 nm, are observed evenly dispersed into the polymeric surface layer [Fig. 1(b)]. In addition, a continuous microcrack is also detected. On the contrary, almost no microvoids resembling those in Figure 1(b) are detected for PPVC [Fig. 1(e)] at the same aging time. However, its surface layer shrinks evidently. With further increasing the aging time to 8 h, apparently different morphologies for UPVC and PPVC are seen. In the case of the UPVC, the earlier microvoids disappear; meanwhile, many cracks (1–2.5 μm wide) appear [Fig. 1(c)]. For the PPVC, the shrinkage of the surface is invisible, and ample microvoids (100–300 nm) and a few cracks are detected. By comparing Figure 1(a–c) with Figure 1(d–f), it is concluded that the aging process of both the UPVC and PPVC experiences the change of topology from a smooth state to a rough state, and then follows a growth of defect from microvoids to cracks. Moreover, it also evidently shows that the aging rate of UPVC is relatively higher than that of PPVC, taking account of the fact that SEM micrographs clearly reveal that cracks of the UPVC [Fig. 1(c)] have already extended from the surface layer into deeper layers, whereas microvoids of the PPVC are just of presence [Fig. 1(f)].

ATR-FTIR analysis

ATR-FTIR spectra of the UPVC and PPVC with different aging time are shown in Figures 2 and 3, respectively. As illustrated in Figure 2(a), the characteristic peaks at around 1710 and 1739 cm^{-1}, assigned to carbonyl groups,[14,15] is found to change considerably with the aging time ranges from 0 to 8 h, indicating that some oxygen-containing groups are gradually formed with increasing the aging time. Furthermore, the band at around 1388 and 1427 cm^{-1}, assigned to the $-CH_2-$ group, is also detected to dramatically change with aging time [Fig. 2(b)], implying the occurrence of dehydrochlorination during the aging process. In the case of the PPVC (Fig. 3), the characteristic peak at around 1720 cm^{-1}, assigned to the carbonyl groups of phthalate, noticeably widens with aging time. Moreover, another $-C=O$ asymmetric vibration at near 1750 cm^{-1} is observed, and its intensity slightly increases with aging time. A similar tend of the $-CH_2-$ group resembling that of UPVC is seen for PPVC as well. However, such change is relatively slight.

UV–visible results

To further study the dependence of chemical structure of PVC polymeric chains on aging time, an UV–visible spectrometer is used, and the corresponding

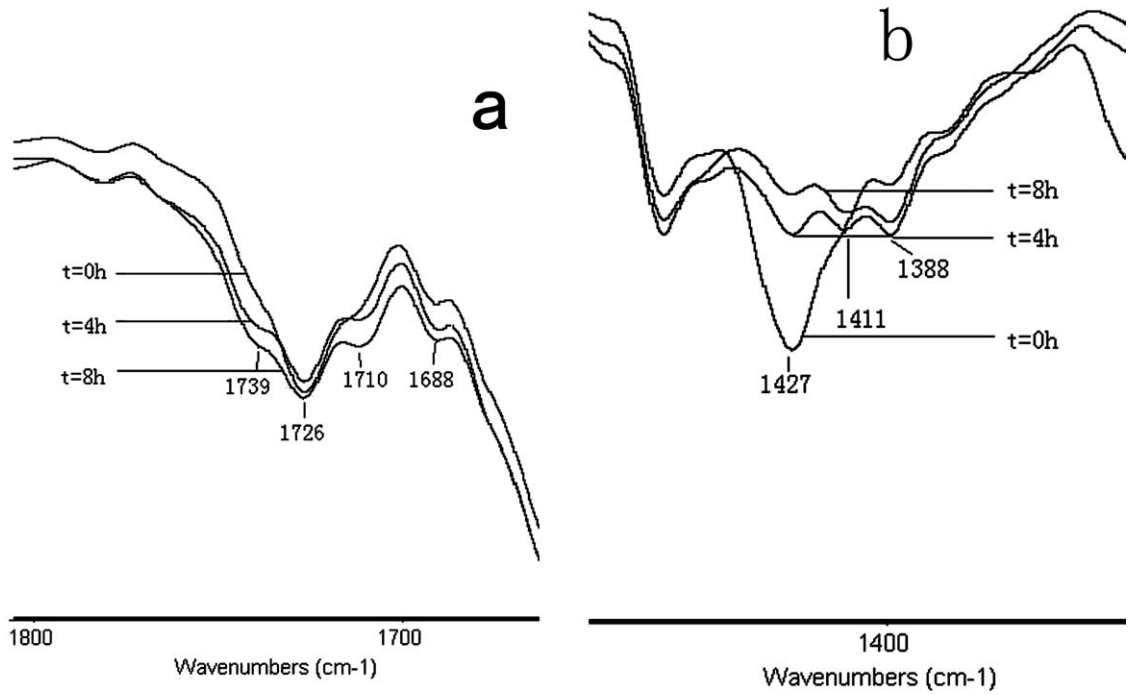

Figure 2 ATR-FTIR spectra of UPVC with different aging time.

results are shown in Figure 4 for UPVC and Figure 5 for PPVC, respectively. In Figure 4, there are only two absorption peaks at around 280 and 331 nm in the range of 400–800 nm for the un-aged sample, revealing a low conjugation along the PVC polymeric chains. However, some absorption peaks at around 280, 450, 550, and 750 nm, originated from conjugated groups or conjugated segments along the polymeric chains are apparently observed. Especially, the bands at around 450, 550, and 750 nm,

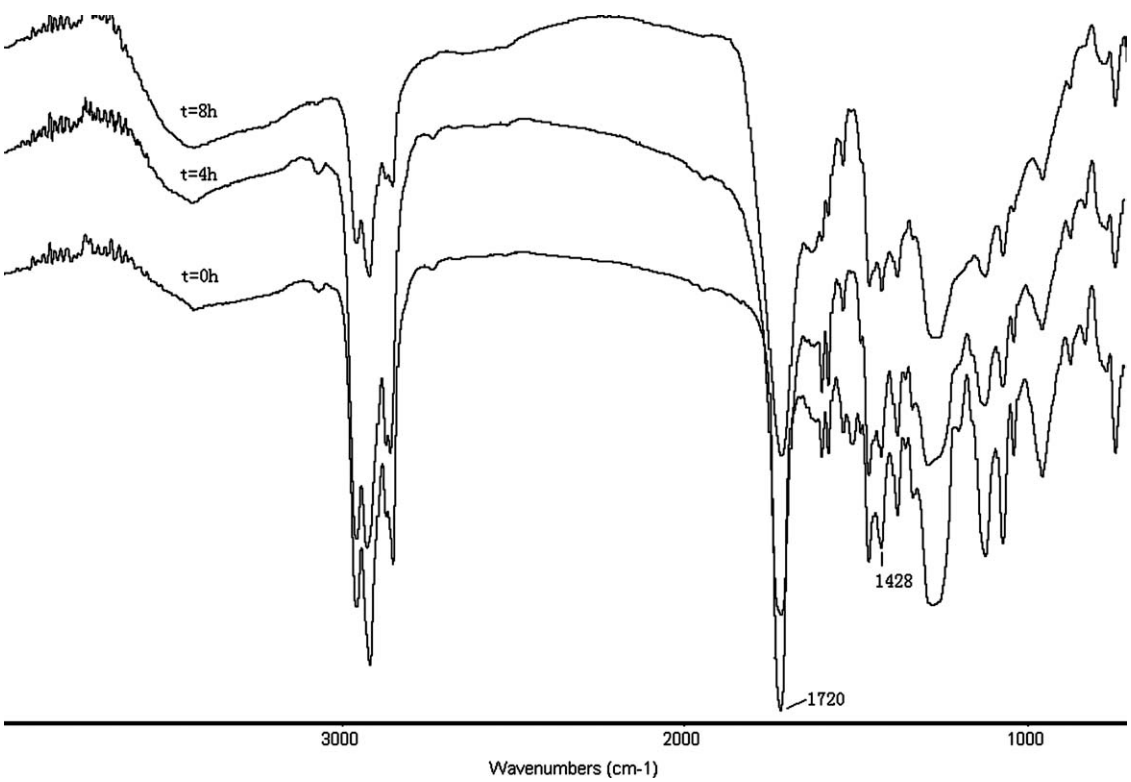

Figure 3 ATR-FTIR spectra of PPVC with different aging time.

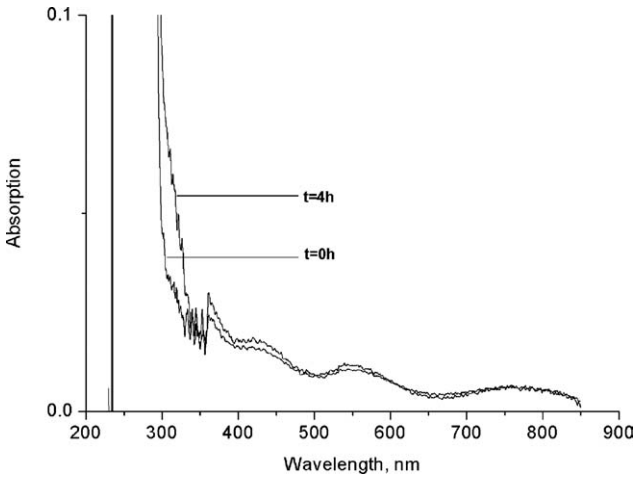

Figure 4 UV spectra of UPVC with different aging time.

derived from longer conjugated segments, are detected to gradually increase with aging time rising from 0 to 8 h, implying the occurrence of dehydrochlorination. In the case of PPVC (Fig. 5), absorption peaks at near 360, 420, 550, and 760 nm are seen for the neat sample. After a certain aging time, e.g., 4 h, the earlier absorption peaks are almost unchanged, revealing the absence of dehydrochlorination and PPVC having a good antiaging capacity.

GPC results

Table III demonstrates the change of average MW of sample with aging time. It clearly shows that MW of both the UPVC and PPVC does not alter significantly with increasing the aging time. A slight increase of MW from 9.52×10^4 to 9.98×10^4 is detected for UPVC as the aging time reaches 4 h, namely, about a 4.8% increment of MW. It can be accounted for the fact that UPVC degradation is initiated by the scission of C—Cl bond, and then the crosslinking reaction between two macromolecular free radicals, derived

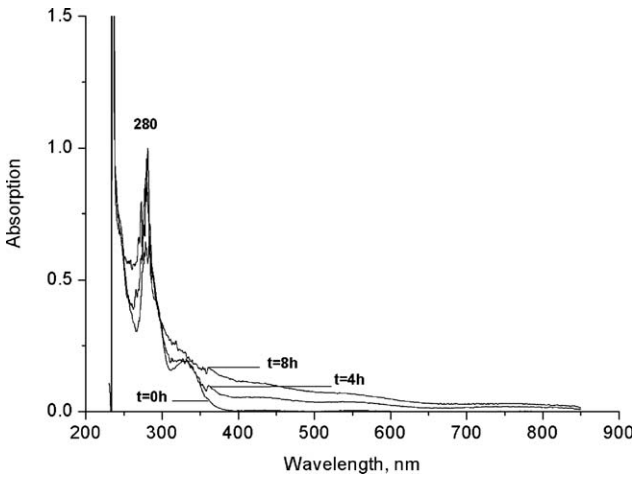

Figure 5 UV spectra of PPVC with different aging time.

TABLE III
Effect of Aging Time on the Average Molecular Weight

	UPVC			PPVC		
Aging time (h)	0	4	8	0	4	8
$M_n \times 10^4$ (g/mol)	9.52	9.98	7.43	10.30	9.87	8.44

from the dehydrochlorination reaction, is likely to occur,[16] which directly lead to the increase of MW. However, MW sharply reduces by about 22% when the aging time increases to 8 h. In the case of PPVC, its MW steadily decreases by about 4% at the aging time of 4 h, and then reduces again by about 14% at the aging time of 8 h. Combining the trend MW changing with the corresponding morphologies, it evidently reveals that an accelerating aging process is prone to occur once microvoids or microcracks are formed in the surface layer, namely the formation of a relatively rough topology.

Tensile tests

Tensile strength and elongation at break of the sample with aging time are shown in Figures 6 and 7 for UPVC and PPVC, respectively. It reveals in Figure 6 that the tensile strength gradually enhances from 55.2 MPa to a maximum of 55.8 MPa at the aging time range of 0–4 h, and then slightly reduces from the maximum to 50.8 MPa as the aging time alters from 4 to 8 h, and that the elongation at break steeply decreases from 35% to 21% at the beginning of aging time range (0–2 h), and from 21% to 12.5% within the following 6 h. The corresponding reduction of the tensile strength at 4 and 8 h approaches −1% and 8%, respectively. Although the decrements of the elongation at break at earlier aging time achieve 42% and 67%, respectively. In the case of PPVC (Fig. 7), the tensile strength of the specimen only reduces from 16.2 to 15.6 MPa at the aging time range of 0–4 h, and then almost keeps in a constant

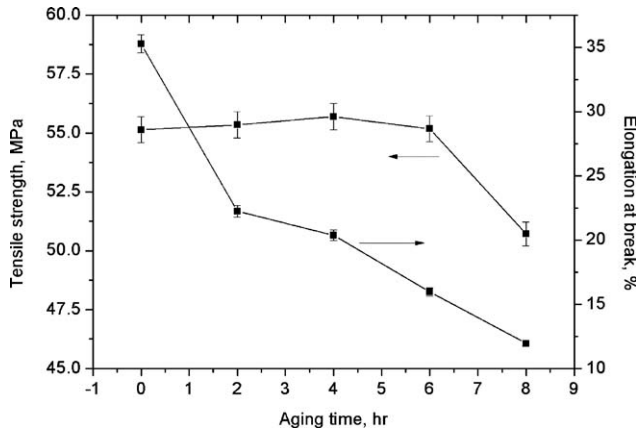

Figure 6 Tensile strength and elongation at break of UPVC with different aging time.

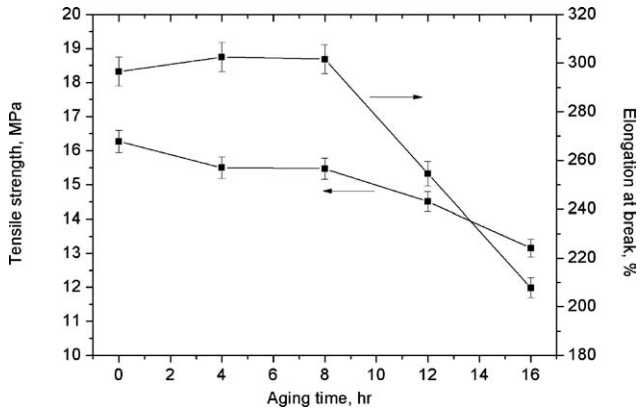

Figure 7 Tensile strength and elongation at break of PPVC with different aging time.

at the aging time range of 4–8 h. Subsequently, it sharply decreases to 13 MPa with further increasing the aging time from 8 to 16 h. Correspondingly, the value of the elongation at break of the sample at the aging time range of 0–8 h is almost equal to that at the aging time of 0 h, namely the un-aged PPVC. It steeply reduces from 304% to 210% when the aging time further increases from 8 to 16 h, showing a similar variety tendency with the tensile strength plot. Especially, it is apparent that at the same aging time, for instance, 8 h, UPVC is more likely to be degraded than PPVC because the conservation capacity of the comprehensive properties of PPVC is evidently higher than that of UPVC.

By comparing the earlier tensile properties with GPC results, it is presumably concluded that both the increment of the tensile strength and the reduction of the elongation at break of UPVC before the aging time of 6 h is attributed to the enhancement of MW, deriving form the crosslinking reactions between different segmental free radicals. In the case of PPVC, the change of tensile strength and elongation at break is also due to MW change with the aging process.

Formation mechanism of microvoids and microcracks

It is convinced that the formation of surface defects during aging is mainly originated from the elimination of inorganic fillers, processing additives, and plasticizers, and from the aggregation of molecular chains in the interfacial layer.[17–20] Unfortunately, such viewpoint seems unfeasible for the systems without the earlier mentioned materials, e.g., neat PVC. Therefore, a deeper investigation regarding the formation mechanism of microvoids and microcracks accompanying the aging process is indispensable. In this article, for further understanding the formation mechanism of microvoids and microcracks of both the UPVC and PPVC, the nearly adjacent regions of microcracks have been primarily characterized. Moreover, the thermodynamic reason corresponding to the formation of microvoids and microcracks are extensively evaluated as follows.

From the thermodynamic and classical mechanics points of view, it is evident that the total Gibbs energy and resultant force of a general composite system at an ideal equilibrium condition [e.g., certain temperature (T), pressure (P), and volume (V)] are zero,[21] i.e.,

$$\sum \Delta G = \sum \Delta H - T \cdot \sum \Delta S = 0 \tag{1}$$

$$\sum F_{P,V,T} = 0 \tag{2}$$

In this article, if we assume that the systematic temperature, pressure, and volume of sample are unchanged with aging process, and that the Gibbs energy and resultant force simultaneously changes when the dehydrochlorination occurs and when the conjugated segments and polar groups containing oxygen are formed, i.e.,

$$\Delta G_d = \Delta H_d - T \cdot \Delta S_d \neq 0 \tag{3}$$

$$\Delta G_c = \Delta H_c - T \cdot \Delta S_c \neq 0 \tag{4}$$

$$\Delta G_p = \Delta H_p - T \cdot \Delta S_p \neq 0 \tag{5}$$

$$\sum \Delta G = \sum \Delta G_i = \Delta G_d + \Delta G_c + \Delta G_p + \ldots \neq 0, (i = d, c, p \ldots) \tag{6}$$

where the subscript letters d, c, and p stand for the dehydrochlorination, formation of conjugated segments, and polar groups containing oxygen, respectively.

Therefore, if the value of ΔG_i ($i = d, c, p, \ldots$) is available, the instantaneous systematic Gibbs energy at an equilibrium phase can be obtained, and the resultant force dependence of the instantaneous systematic Gibbs energy can be also elicited according to the classical Newton mechanics as follow:

$$W = \int_0^{\varepsilon_1} \sum F_{P,V,T} \cdot dl = \sum \Delta E \tag{7}$$

On the basis of what have been discussed above, the energy change between every two phases should be obtained to develop the quantitative relationship between energy and defects (microvoids). Herein, for simplicity, it seems feasible to approximately consider the entire integral times (N_i) of cohesion energy (ΔE_i) of groups as energy change between every two phases, i.e.,

$$\sum \Delta G_i \approx \sum N_i \cdot \Delta E_i \neq 0 (i = d, c, p \ldots) \tag{8}$$

TABLE IV
Cohesion Energy of Some Typical Groups

Group	CE (kJ/mol)	Group	CE (kJ/mol)
—CH_2—	2.84	—COOH	23.4
—O—	4.18	—OH	24.2
—CH_3—	7.11	—NHCO—	35.5
—CO—	11.12	—NHCOO—	36.4
—COO—	12.1	—NHCONH—	>36.5
—Phenyl	16.3		

$$W = \int_0^{\varepsilon_1} \sum F_{P,V,T} \cdot dl = \sum \Delta E = \sum \Delta G_i \approx \sum N_i \cdot \Delta E_i \neq 0 (i = d, c, p \ldots) \quad (9)$$

Table IV lists the cohesion energy of some typical groups.[22] The relevant data evidently shows that the cohesion energy of some polar groups containing oxygen, such as carbonyl, ketone, acid, aldehyde, hydroxide, etc., is significantly higher than that of the groups without oxygen. It clearly reveals that all the instantaneous Gibbs energy values of dehydrochlorination and the formation of conjugated segments and polar groups are not zero, and that the energy consumption of dehydrochlorination is remarkably lower than that of the formation of conjugated segments and polar groups. Thus, there will be an energy gap (E_g), whose value is not zero, between dehydrochlorination and the formation of conjugated segments and polar groups. In addition, such an energy gap will directly result in changing the molecular conformation or forming the inner stress, or both of them, to obey the total Gibbs energy law of eq. (1).

Therefore, if we mark the energy consumption of the change of molecular conformation as E_m, the residual energy E_r can be elicited,

$$E_r = E_g - E_m \quad (10)$$

$$E_g = \sum \Delta G_i \approx \sum N_i \cdot \Delta E_i (i = d, c, p \ldots) = N_d \Delta E_d + N_c \Delta E_c + N_p \Delta E_p + \ldots \neq 0 \quad (11)$$

$$E_m = \int_0^{\varepsilon_1} \sum F_{P,V,T} \cdot dl (i = d, c, p \ldots) \quad (12)$$

$$E_r = \sum N_i \cdot \Delta E_i - \int_0^{\varepsilon_1} \sum F_{P,V,T} \cdot dl \neq 0 (i = d, c, p \ldots) \quad (13)$$

In the case of the UPVC, the polymeric main chains are not flexible to change their conformations to counteract the energy originated from the comprehensive effect of both the dehydrochlorination and the formation of conjugated segments and polar groups, taking account of the relatively high glass transition temperature of polymeric chains. Consequently, the value of ε_1 in eq. (12) is close to zero, and the resultant force is remarkably larger than zero.

$$E_m = \int_0^{\varepsilon_1} \sum F_{P,V,T} \cdot dl = \sum \sum F_{P,V,T} \cdot \varepsilon_1 \to 0 \quad (14)$$

$$\sum F_{P,V,T} \cdot \varepsilon_1 = E_m \Big/ \sum \varepsilon_1 \gg 0 \quad (15)$$

Subsequently, to conform to eq. (1),

$$\sum \Delta G = \sum \Delta H - T \cdot \sum \Delta S \to 0 \quad (16)$$

$$\sum \Delta G_v - E_r = 0 \quad (17)$$

$$\int_0^{\varepsilon_2} \sum F_{P,V,T} \cdot dl = \sum N_i \cdot \Delta E_i - \int_0^{\varepsilon_1} \sum F_{P,V,T} \cdot dl \quad (18)$$

$$\int_0^{\varepsilon_1} \sum F_{P,V,T} \cdot dl \to 0, (\varepsilon_1 \to 0) \quad (19)$$

$$\int_0^{\varepsilon_2} \sum F_{P,V,T} \cdot dl \approx \sum N_i \cdot \Delta E_i \neq 0, (i = d, c, p \ldots) \quad (20)$$

$$\varepsilon_2 > 0 \quad (21)$$

Therefore, many microvoids are formed ($\varepsilon_2 > 0$) due to the impulse of large stress ($\sum F_{P,\,V,\,T}\ 5 \gg 0$).

In the case of the PPVC, the polymeric main chains can flexibly adjust their conformations and counteract plenty of energy by heat consumption, due to the fact that T_g of PPVC is significantly lower than the aging temperature, and that the friction of both the intermolecular and intramolecular chains directly leads to the energy consumption in the form of heat. Therefore, at the beginning of the aging process, ε_1 in eq. (23) is remarkably larger than zero ($\varepsilon_1 \gg 0$), attributing to the flexibility of PPVC molecular chains. Subsequently, the inner stress gradually reduces with aging time, originating from the energy consumption of segmental motions, and then ε_2 increases correspondingly. The relevant elicitation is shown as follows:

$$\varepsilon_1 \gg 0 \quad (22)$$

$$E_m = \int_0^{\varepsilon_1} \sum F_{P,V,T} \cdot dl = \sum \sum F_{P,V,T} \cdot \varepsilon_2 \gg 0 \quad (23)$$

$$\sum \Delta G = \sum \Delta H - T \cdot \sum \Delta S \to 0 \quad (24)$$

$$\sum \Delta G_v - E_r = 0 \quad (25)$$

$$\int_0^{\varepsilon_3} \sum F_{P,V,T} \cdot dl = \sum N_i \cdot \Delta E_i - \int_0^{\varepsilon_1} \sum F_{P,V,T} \cdot dl \quad (26)$$

$$\int_0^{\varepsilon_1} \sum F_{P,V,T} \cdot dl \gg 0 (\varepsilon_1 \gg 0) \quad (27)$$

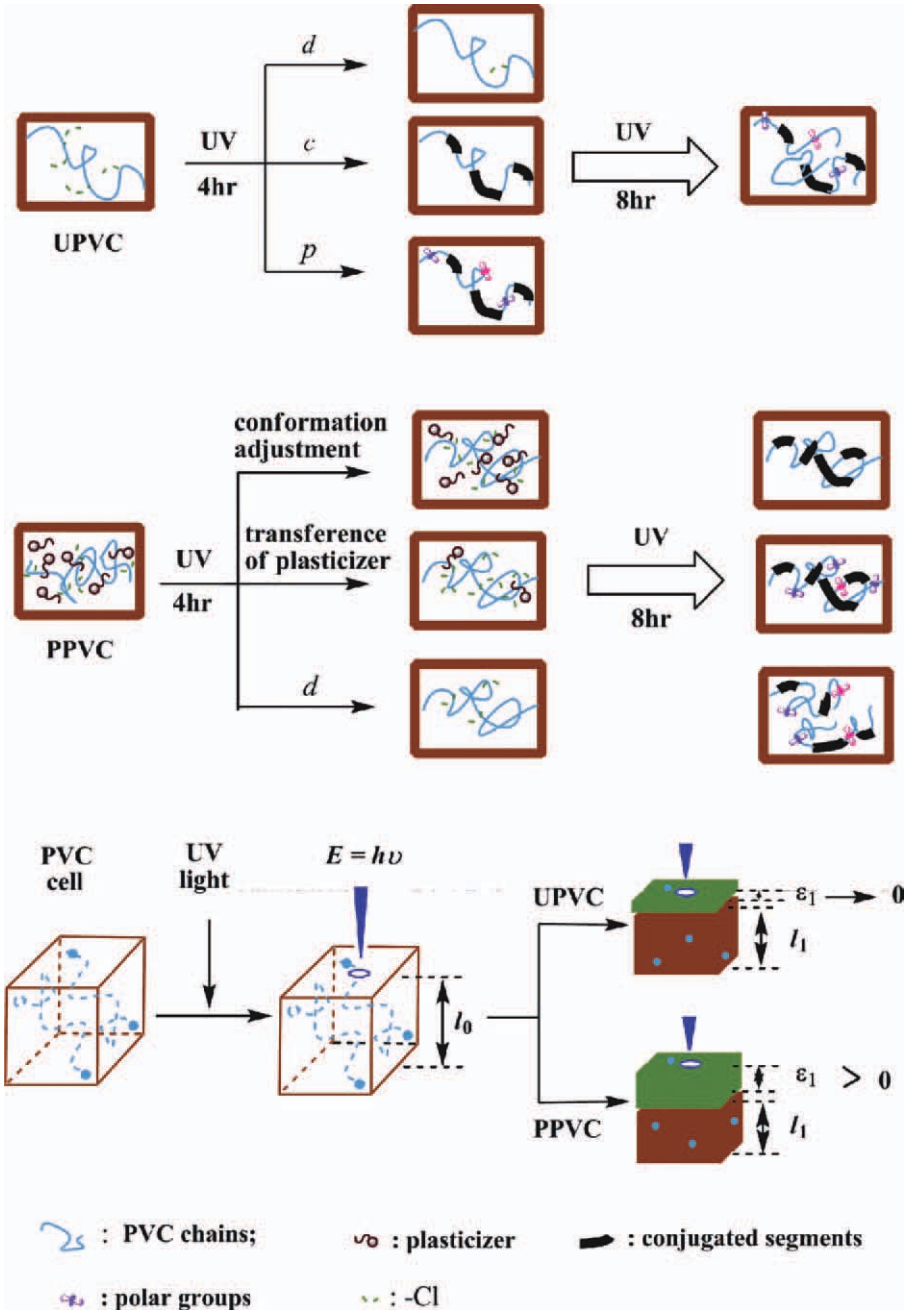

Scheme 1 Schematic formation mechanism of microvoids and microcracks under accelerating aging conditions. [Color figure can be viewed in the online issue, which is available at wileyonlinelibrary.com.]

$$\int_0^{\varepsilon_3} \sum F_{P,V,T} \cdot dl = \sum N_i \cdot \Delta E_i - \int_0^{\varepsilon_1} \sum F_{P,V,T} \cdot dl \ll \sum N_i \cdot \Delta E_i \quad (28)$$

$$0 < \varepsilon_3 < \varepsilon_2 \quad (29)$$

The earlier elicitation semiquantitatively shows that the length of microvoids of UPVC (ε_2) is far larger than that of PPVC (ε_3) at the same aging time, which is in good accordance with the experimental results shown in the SEM section. The relevant mechanism can be briefly shown in scheme 1.

In addition, microcracks are further formed from microvoids with persistent artificial aging process, due to the fact that the residual energy E_r in eq. (13) is still larger than 0.

CONCLUSIONS

The aging process of both the UPVC and PPVC experiences an initiation of microvoids, and then follows the increase of both the number and length of microvoids and the gradual formation of microcracks. FTIR and UV spectroscopy demonstrate that

the formation of original microvoids has accompanied with the appearance of many polar groups containing oxygen. Average MW and its distribution of both the PVC samples slightly changes with aging time. Thermodynamic analysis of the aging process reveals that the generation and growth of microvoids are attributed to the relaxation of residual energy of system, deriving from the comprehensive effects of dehydrochlorination, creation of polar groups, and the adjustment of conformation of macromolecular chains.

REFERENCES

1. Purmova, J.; Pauwels, K. F. D.; Zoelen, W. V.; Vorenkamp, E. J.; Schouten, A. J. Macromolecules 2005, 38, 6352.
2. Sun, Q.; Zhou, D. S.; Wang, X. L.; Xue, G. Macromolecules 2002, 35, 7089.
3. Wang, J. L.; Yang, W. Q.; Lei, J. X. Polym Eng Sci 2010, 50, 57.
4. Dunn, P.; Oldfield, D.; Stacewicz, R. H. J Appl Polym Sci 1970, 14, 2107.
5. Garcia, J. C.; Marcilla, A. Polymer 1998, 39, 3507.
6. Audourin, L.; Dalle, B.; Metzger, G.; Verdu, J. J Appl Polym Sci 1992, 45, 2091.
7. Audourin, L.; Dalle, B.; Metzger, G.; Verdu, J. J Appl Polym Sci 1992, 45, 2097.
8. Bengough, W. I.; Vermna, I. K. Eur Polym J 1966, 2, 61.
9. Mitani, K.; Ogawa, T. J Appl Polym Sci 1974, 18, 3205.
10. Liebman, S. A.; Foltz, C. R.; Reuwer, J. F.; Obremski, R. J. Macromolecules 1971, 4, 134.
11. Ito, M.; Nagai, K. Polym Degrad Stab 2007, 92, 260.
12. Shashoua, Y. R. Polym Degrad Stab 2003, 8, 129.
13. Gesenhues, U. Polym Degrad Stab 2000, 68, 185.
14. Gonzalez, N.; Fernandez-Berridi, M. J. J Appl Polym Sci 2006, 101, 1731.
15. Starnes, W. H. J.; Schiling, F. C.; Abbas, K. B.; Plitz, I. M.; Hartless, R. L.; Bovey, F. A. Macromolecules 1979, 12, 13.
16. Biggin, I. S.; Gerrard, D. L.; Williams, G. E. J Viny Tech 1982, 4, 150.
17. Bacaloglu, R.; Fisch, M. Polym Degrad Stab 1995, 47, 33.
18. Kaminska, A. Angew Makromol Chem 1982, 107, 43.
19. Duvis, T.; Karles, G.; Papaspyrides, C. D. J Appl Polym Sci 1991, 42, 191.
20. Jayabalan, M. Angew Makromol Chem 1986, 139, 33.
21. Lu, X. Y.; Liu, J. L.; Feng, M., Eds. Physical Chemistry; Chemical Industry Press: Beijing, 2008; p 64 [in Chinese].
22. Li, S. X.; Liu, Y. J., Eds. Polyurethane Resin and Its Application; Chemical Industry Press: Beijing, 2002; p 43 [in Chinese].